Switching mode photovoltaic pumping system

Wagdy R. Anis
Electronic & Communication Department, Faculty of Engineering, Ain Shams University, 1 Sarayat Street, Abbasia, Cairo (Egypt)

M. Abdul-Sadek Nour*
Yanbu Industrial College, Electronic Department, P.O. Box 30436, Yanbu AL-sinaiyah 21477 (Saudi Arabia)

(Received April 29, 1993; accepted May 28, 1993)

Abstract

Photovoltaic (PV) pumping systems are widely used due to their simplicity, high reliability and low cost. A directly-coupled PV pumping system is the most reliable and least-cost PV system. The d.c. motor-pump group is not, however, working at its optimum operating point. A battery buffered PV pumping system introduces a battery between the PV array and the d.c. motor-pump group to ensure that the motor-pump group is operating at its optimum point. The size of the battery storage depends on system economics. If the battery is fully charged while solar radiation is available, the battery will discharge through the load while the PV array is disconnected. Hence, a power loss takes place. To overcome the above mentioned difficulty, a switched mode PV pumping is proposed. When solar radiation is available and the battery is fully charged, the battery is disconnected and the d.c. motor-pump group is directly coupled to the PV array. To avoid excessive operating voltage for the motor, a part of the PV array is switched off to reduce the voltage. As a result, the energy loss is significantly eliminated. Detailed analysis of the proposed system shows that the discharged water increases by about 10% when compared with a conventional battery-buffered system. The system transient performance just after the switching moment shows that the system returns to a steady state in short period. The variations in the system parameters lie within 1% of the rated values.

Introduction

PV pumping systems have been discussed in many publications [1–5]. Appelbaum and Bany [1, 2] have analysed directly-coupled PV pumping systems. Roger [3] has proved that the characteristics of the centrifugal pump are well matched with PV arrays. Thus, a directly-coupled d.c. motor-centrifugal-pump group extracts most of the available solar energy generated by the PV array. The coupling of the d.c. motor-volumetric-pump group is discussed in ref. 4. Although the directly-coupled system is the least-cost and most reliable system, the d.c. motor-pump group is not operating at the optimum point and, consequently, some energy loss is incurred. A battery-buffered pumping system [5] eliminates the previously mentioned difficulty by connecting a storage battery between the PV array and the d.c. motor-pump group. Hence, the motor is operating at its maximum efficiency point. For a battery-buffered system,

*Author to whom correspondence should be addressed.

there are two types of loss. First, there is an energy loss in the battery, since the output energy supplied by the battery is about 80% of the stored energy, this energy loss is inevitable. Second, there is an energy loss due to the array disconnect when the storage battery is fully charged. Under this condition, the load is supplied through the battery while the available solar energy is wasted. Thus, it is clear that the PV array disconnect causes a double energy loss, namely, the available solar energy by disconnecting the PV array and the stored energy in the storage battery.

In this work, a switched-mode PV pumping system is proposed. This system makes use of the advantages of both battery-buffered and directly-coupled systems. The system is basically a battery-buffered unit, but when the battery is fully charged the load is directly coupled to the PV array. By this technique, the available solar energy is used optimally.

System description

The system proposed is composed of a modular PV array, a storage battery, a permanent magnet d.c. motor driving a centrifugal pump, and a battery voltage regulator (BVR), as shown in Fig. 1.

The switches S_1, S_2 and S_3 are controlled by the BVR circuit. The parameter that determines the mode of operation of the system is the state-of-charge (SOC) of the battery. The battery should be disconnected if the SOC falls either below a minimum value limit, (SOC_{min}) to avoid heavy discharge of the battery, or rises above a maximum SOC_{max}, to avoid overcharging of the battery. Table 1 summarizes the operating conditions of the system.

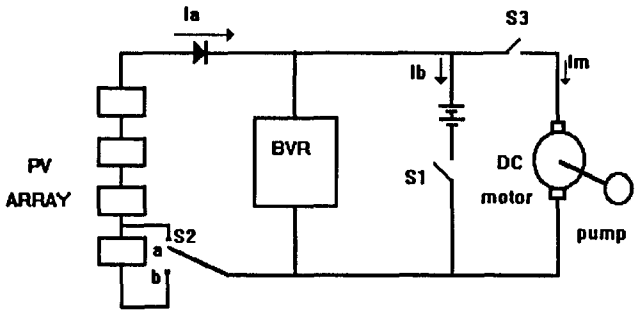

Fig. 1. Schematic representation of the proposed system.

TABLE 1

Operating conditions of the proposed system

State	Condition	Switch		
		S_1	S_2	S_3
1	$SOC_{min} > SOC > SOC_{max}$	closed	in position b	closed
2	$I_a < I_m$ and $SOC < SOC_{min}$	closed	in position b	opened
3	$I_a > I_m$ and $SOC > SOC_{max}$	opened	in position a	closed

When the array current I_a is greater than the motor current I_m and the battery is fully charged (i.e., $SOC > SOC_{max}$), the load is directly coupled to the array. To avoid excessive operating voltage, a part of the array is disconnected. This is achieved by connecting the switch S_2 to position a.

If I_a is $< I_m$ and SOC is $< SOC_{min}$, the load is disconnected (i.e., S_3 is opened) to prevent heavy discharge of the battery. The previous described mode of operation protects the battery and prolongs its life time.

The normal operation conditions of the system is state 1 in Table 1. This is the case of a battery-buffered mode of operation. In this situation, the battery may be charging or discharging. If I_a is $> I_m$, then the battery is charging and $I_b = I_a - I_m$. When I_a is $< I_m$, the battery is discharging and $I_b = I_m - I_a$. Thus, I_b (as indicated in Fig. 1) may be positive (in the case of charging the battery) or negative (in the case of discharging the battery).

The motor current I_m is determined by the mechanical load that is being driven by the motor. In other words, the mechanical torque of the load determines I_m. The array current I_a is determined by the instantaneous insolation.

System modelling

The three basic units of the system are: (i) PV array; (ii) d.c. motor-pump group; (ii) storage battery. These units are modelled hereafter.

PV array current/potential characteristics

The array current I_a is given by:

$$I_a = I_{Lo} G - I_o \exp[(V + I_a R_s)/V_T - 1] - (V + I_a R_s)/R_{sh} \quad (1)$$

where: I_a is the array current (A); I_{Lo} is the light generated current at insolation $G =$ 1 kW m^{-2} (A); G is the global insolation on array surface (kW m^{-2}); I_o is the array reverse saturation current (A); V is the array terminal voltage (V); R_s is the array series resistance (Ω); V_T is the array thermal voltage (V); R_{sh} is the array shunt resistance (Ω).

The global insolation G is determined by the technique described in ref. 6. The array reverse saturation current I_o is related to the operating temperature T_c of the solar cells by [7]:

$$I_o = A_o (273 + T_c)^3 \exp[-E_{Go}/K(T_c + 237)] \quad (2)$$

where: A_o is a constant; E_{Go} is the energy gap of the material of the solar cells; T_c is expressed in °C.

D.c. motor-pump group characteristics

If a voltage V is applied across the permanent magnet (constant flux) d.c. motor, the motor performance is given by:

$$V = I_m R_a + K_m \omega \quad (3)$$

$$T_m = K_m I_m \quad (4)$$

$$(V - I_m R_a) I_m = T_m \omega \quad (5)$$

where: I_m is the d.c. motor armature current. Note that for a permanent magnet motor the field current is zero and, consequently, the armature current is the total motor

current; R_a is the d.c. motor armature resistance; K_m is the constant for a given d.c. motor; ω is the angular speed of the d.c. motor; T_m is the torque developed by the d.c. motor.

Neglecting the rotational loss of the d.c. motor, the load torque T_L can be equated to the torque developed by the d.c. motor that is driving the load. For a centrifugal pump, the torque is proportional to the square of the angular speed [8], thus:

$$T_m = T_L = K_p \omega^2 \tag{6}$$

where K_p is a pump constant. Water discharge Q is determined by the water head, H, and the pump efficiency, η_p, i.e.:

$$Q\rho H = \eta_p T_L \omega \tag{7}$$

where: g is the gravitational acceleration (9.8 m s^{-2}); ρ is the water density (kg m^{-3}).

Battery characteristics

The characteristics of storage lead/acid batteries are described in ref. 10. During charging, the SOC of the battery is given by:

$$SOC = SOC_0 - \eta_{ch}(I_b t_{ch}/Ah) \tag{8}$$

where: SOC_0 is the initial state-of-charge; I_b is the battery charging current; t_{ch} is the charging period; Ah is the battery capacity in ampere-hours; η_{ch} is the charging efficiency.

The battery voltage V_B during charging is given by:

$$V_B = V_{Bo}\{1 + (I_b/Ah)[(0.189/(1.142 - SOC) + 0.15)]\} \tag{9}$$

where V_{Bo} is the nominal voltage, for lead/acid batteries, i.e., $V_{Bo} = 2.094\ n$ volts, where n is the number of battery cells that are connected in series. During discharging:

$$SOC = SOC_0 - (I_b t_{dis}/Ah\ \eta_{dis}) \tag{10}$$

where t_{dis} is the discharge period and η_{dis} is the discharge efficiency. During the discharging period, V_B is given by:

$$V_B = V_{Bo}\{1 - (I_b/Ah)[(0.189/SOC + 0.15)]\} \tag{11}$$

If SOC exceeds 90%, V_B is determined by:

$$V_B = V_{Bo}\{1 + (I_b/Ah)[(0.189/(1.142 - SOC) + 0.15)] + (SOC - 0.09)\ \ln[(300\ I_b/Ah) + 1]\} \tag{12}$$

Transient response of the system

At the moment when switch S_2 (in Fig. 1) changes its contact from point b to point a, switch S_1 is opened and the system changes from a battery-buffered mode of operation to a directly-coupled mode excluding a part of the PV array. As a result, the motor operating voltage changes at this moment. The transients are determined by the following relations [9]:

$$V = K_m \omega + I_m R_a + L_a dI_m/dt \tag{13}$$

$$T_m = J d\omega/dt + K_m I_m \tag{14}$$

where: L_a is the armature inductance; J is the moment of inertia.

During the transient period, the d.c. motor-pump group is directly coupled to the PV array. Thus, $I_a = I_m$ and eqn. (1) may be written as:

$$I_m = I_{Lo}G - I_o\{\exp[(V+I_mR_s)/V_T] - 1\} - (V+I_mR_s)/R_{sh} \quad (15)$$

Equations (13), (14) and (15) are solved numerically to obtain the variables V, I_m and ω as functions of time. The initial conditions are the values of V, I_m and ω at the last moment before switch S_2 moves from position b, while the system is operating in battery-buffered mode.

System design criterion

The final objective of the design of a pumping system is the minimization of the cost of pumping of one cubic meter from a given depth.

The major costs of the PV-powered pumping system are those associated with the [10]:

(1) PV array, including its installation;
(2) battery storage and BVR;
(3) d.c. motor-pump group;
(4) well digging and pump installation, and
(5) installation of the water storage tank and piping distribution system.

Enlarging the PV array and battery storage size allows water pumping during both the day and the night. It is obvious that enlarging the PV array and the battery storage will increase the system cost but, on the other hand, the amount of pumped water will increase. By contrast, a small PV array and a small size of battery will reduce the system cost, but the amount of pumped water will also be reduced. The items (1) and (2) of the system costs are directly proportional to the PV array size, while the costs of items (3), (4) and (5) are independent of the array size. If the costs of (3), (4) and (5) are the major costs, then enlarging the PV array and battery storage leads to minimum cost per cubic meter of water pumped. On the other hand, if the costs of (1) and (2) are the major costs, then a battery system with minimum array and battery sizes leads to minimum cost per cubic meter of pumped water. Under these conditions, a directly-coupled system will be the optimum unit.

The analysis given hereafter relates to a system with a large PV array and a storage battery where the costs (3), (4) and (5) are the major costs.

Results

The results are obtained for a pumping system operating in Cairo city (Egypt), 30° N. The d.c. motor rating is 48 V and 20 A.

The motor and pump constants are:

$K_m = 0.85$ V s/rad., $R_a = 0.3\ \Omega$, $L_a = 2.2$ mH, $K_p = 0.0051$ Nm s^2, $\eta_p = 83\%$,

and $J = 0.136$ Nm s^2.

The array constant are:

$I_{Lo} = 145$A, $R_s = 0.0414\ \Omega$, $R_{sh} = 20.7\ \Omega$, $I_o = 2.9 \times 10^{-8}$ A (at $T_c = 75$ °C).

The battery capacity is 1550 Ah. The system is designed to pump water continuously day and night to maximize the water discharge. SOC_{min} and SOC_{max} are 0.2 and 0.98, respectively.

To show the advantages of the proposed system, a comparison is made with a conventional battery-buffered system, as shown in Fig. 2. In this system, S_1 and S_2 are closed if $SOC_{min} < SOC < SOC_{max}$. S_2 is opened if $SOC < SOC_{min}$ and $I_a < I_m$. While if $SOC \geq SOC_{max}$, the switch S_1 is opened and the load is supplied by the storage battery I_m. Finally, if $SOC \geq SOC_{max}$, then the switch S_1 is opened and the load is supplied by the storage battery.

Figure 3 shows the daily pumped water, Q_D, throughout a complete year for both the proposed and the conventional battery-buffered system. It is clear that the pumped water of the proposed system is about 10% (on an annual basis) larger than that of the conventional one. Also shown is the amount of water that is pumped during the directly coupled periods Q'_D. It is obvious that Q'_D increases during the summer season when solar radiation is high and the battery is fully charged. Note that the horizontal axis starts with 1 January as day no. 1. The increase in daily discharge of the proposed system is larger than that of the conventional system by an amount that is less than the amount of water discharge during the direct-coupled period. The reason is that during the array disconnect period, the water pumping continues by discharging the battery. The increase in water discharge of the proposed system results

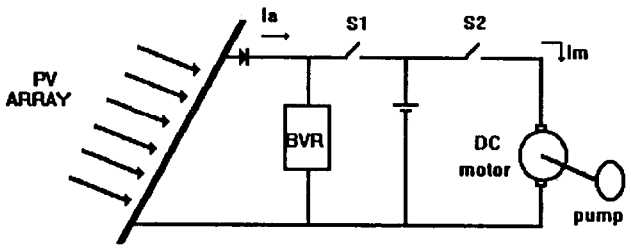

Fig. 2. Conventional buffered system.

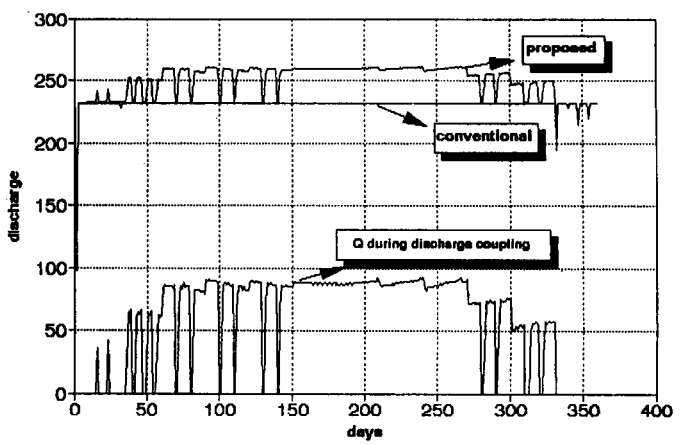

Fig. 3. Daily water discharge for both conventional and proposed systems.

from excess stored energy in the storage battery which increases water pumping during night and cloudy days.

Figure 4 depicts the percentage energy loss due to array disconnect in a conventional system. This energy loss takes place during the summer season when the battery is fully charged. It is clear that the array disconnect amounts to about 40% of the available solar energy in the summer season.

Figure 5 gives the daily variation of SOC for both proposed and conventional systems. It is seen that the SOC of the proposed system is larger than that of the conventional system. It is to be noted that the increase in SOC of the proposed system (compared with the conventional system) is not large. The reason is that both the array and the battery storage are designed with large sizes to ensure continuous water pumping both day and night for the whole year. Hence, the load power is small compared with the array and battery storage sizes. Thus, the saving in energy storage is small compared with battery size.

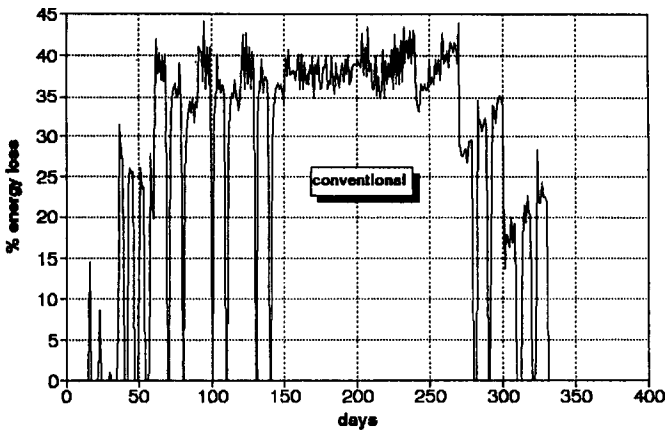

Fig. 4. Percentage energy loss due to array disconnected.

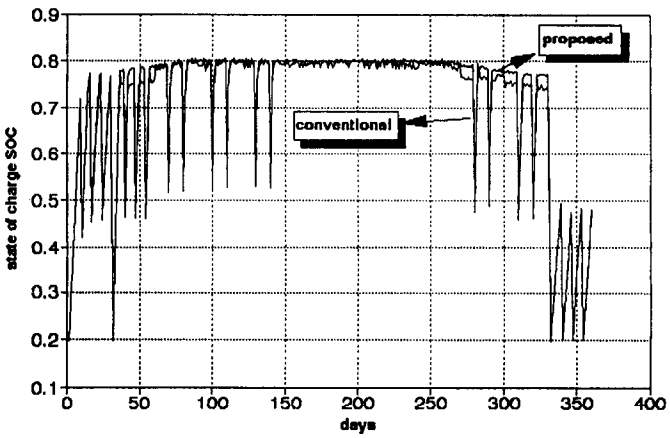

Fig. 5. Battery SOC variations for both conventional and proposed systems.

The transient performance of the system variables just after the switching moment is indicated in Figs. 6–8. The motor speed drops slightly after the switching as shown in Fig. 6, but then returns back to its initial value after a few minutes (not shown in Fig. 6). The whole range of speed variation does not exceed 1% of the rated speed.

Figure 7 shows the variation in the array current, I_a, during the transient period. It is observed that I_a drops by about 0.126% of its initial value and then returns back to its steady-state value.

The voltage rise during the transient period till it reaches the steady-state value as given in Fig. 8. The maximum rise of array voltage is less than 1% of the rated value.

It is seen from Figs. 6–8 that the system reaches its steady-state values within a short period after the switching moment. It is also seen that the system performance varies within 1% of the rated values. The system sensitivity to input parameters such as insolation will be studied in future work.

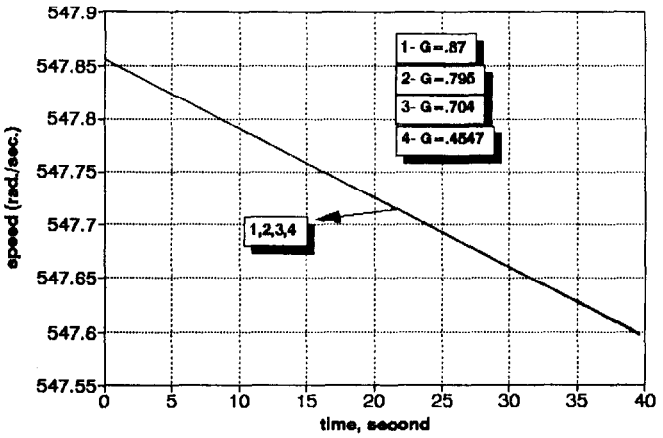

Fig. 6. Speed variation during transient period (for different solar irradiance).

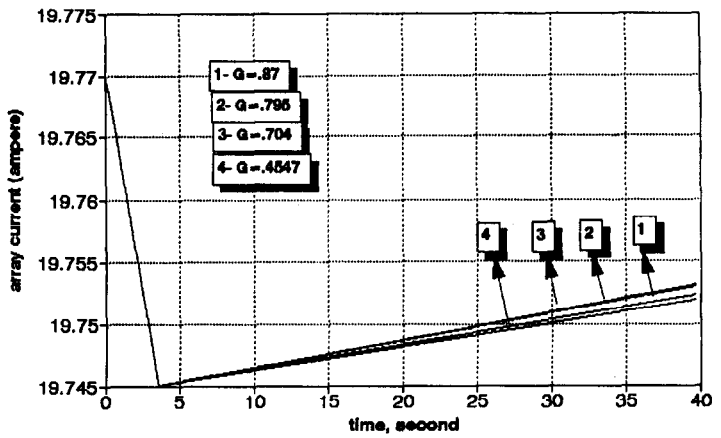

Fig. 7. Variation in array current (I_a) during transient period (for different solar irradiance).

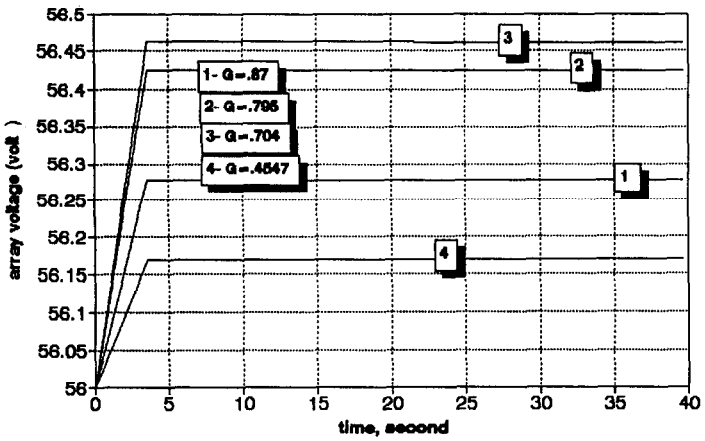

Fig. 8. Variation in array voltage during transient period (for different solar irradiance).

References

1 J. Appelbaum and J. Bany, *1st Commission of the European Communities Conf. Photovoltaic Solar Energy, Luxembourg, Sept. 27–30, 1977,* Reidel, Dordrecht.
2 J. Appelbaum and J. Bany, *Sol. Energy, 22* (1979) 439–445.
3 J. Roger, *Sol. Energy, 23* (1979) 193–198.
4 W.R. Anis, R. Mertens and R. van Overstraeten, *Sol. Cells, 14* (1985) 27–42.
5 W.R. Anis, *Proc. Cairo, Int. Symp. Renewable Energy Sources, Cairo, Egypt, June 13–16, 1988.*
6 S.S. Klein, *Sol. Energy, 19* (1977) 325–329.
7 W.R. Anis, R. Mertens and R. van Overstraeten, *Proc. 5th Commission of the European Communities Conf. PV Solar Energy, Athens, Greece, Oct. 17–21, 1981,* pp. 520–524.
8 M. EL-Hawary, *Principles of Electric Machines with Power Electronic Applications,* Prentice-Hall, Englewood Cliffs, NJ, 1986, Ch. 7.
9 A.E. Fitzgerald, C. Kingsley and M. Kusko, *Electric Machinary,* McGraw-Hill, Tokyo, 3rd edn., 1971, Ch. 9.
10 H.L. Macomber, *Photovoltaic Stand Alone Systems,* Manegan, Gaithersburg, MD, 1981, Ch. 4.